A Multi-scale Friction Model for Sheet Metal Forming Simulations

J.Hol[*], M.V. Cid Alfaro[†], T. Meinders[**] and J. Huétink[**]

[*] *Materials innovation institute (M2i), P.O. box 5008, 2600 GA Delft, the Netherlands*
[†] *Tata Steel Research, Development & Technology, P.O. box 10000, 1970 CA IJmuiden, the Netherlands*
[**] *University of Twente, Faculty of Engineering Technology, chair of Forming Technology, P.O. box 217, 7500 AE Enschede, the Netherlands*

Abstract. This paper presents a multi-scale friction model for large-scale forming simulations based on the surface changes on the micro-scale. The surface texture of a material changes when it is subjected to normal loading and stretching. Consequently, the frictional behavior between contacting surfaces, caused by the adhesion and ploughing effect between contacting asperities, will change when the surface texture changes. A friction model has been developed which accounts for the change of the surface texture on the micro-scale. Statistical parameters have been introduced to make a fast and efficient translation from micro to macro modeling. The flattening models are validated by means of FE simulations on micro-scale and the implementation of the advanced macroscopic friction model in FE codes is discussed.

Keywords: friction, ploughing, adhesion, flattening, roughening, coefficient of friction
PACS: 46.15.-x, 46.35.+z, 46.55.+d

INTRODUCTION

Finite Element (FE) simulations of sheet metal products are everyday practice in the automotive industry. The usability of such a code largely depends on the accuracy of the numerical models in these codes. An accurate forming analysis can only be made if, among others, the material behavior and friction conditions are modeled accurately. For material models, significant improvements have been made in the last decades, but in the majority of simulations still a simple Coulomb friction model is used. Consequently, it is still cumbersome to predict the draw-in and springback of a blank during forming processes correctly.

In the past, research has been carried out on contact and friction phenomena on different length scales. This paper focuses on the phenomena which play a role in the boundary lubrication regime, which is the most common condition during sheet metal forming. On the microscopic level, friction is due to the adhesion and ploughing effect between contacting asperities [1, 2, 3, 4]. The real area of contact, defined as the area summation of contacting asperities, plays an important role in characterizing friction. The real area of contact depends on the roughness of both tool and workpiece, where the roughness of the workpiece is liable to changes due to flattening and roughening mechanisms. The main flattening mechanisms during sheet metal forming are flattening due to normal loading [4, 5, 6, 7, 8] and flattening due to stretching [4, 9, 10]. Flattening increases the real area of contact, resulting in a higher coefficient of friction.

An advanced friction model is proposed which couples the most important friction mechanisms. Based on statistical parameters a fast and efficient translation from micro- to macro modeling is included. A newly developed flattening model, including work hardening effects, has been proposed to describe the increase of real contact area due to normal loading. Asperity flattening due to stretching has been described by the flattening model proposed by Westeneng [4] and the influence of ploughing and adhesion on the coefficient of friction has been described by the friction model of Challen & Oxley [2, 4]. A brief overview of the friction model is presented and the translation from micro to macro modeling is outlined. Next, the theoretical background of the models used to describe the various friction mechanisms are briefly discussed. In the following section, the flattening models are validated by means of FE simulations on the micro-scale. Finally, the implementation of the advanced macroscopic friction model into FE codes is discussed.

The 8th International Conference and Workshop on Numerical Simulation of 3D Sheet Metal Forming Processes
AIP Conf. Proc. 1383, 784-791 (2011); doi: 10.1063/1.3623686

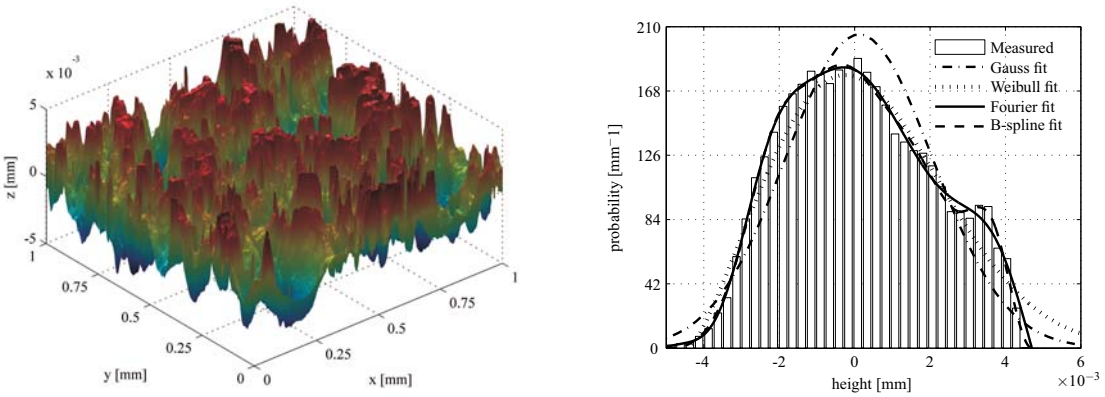

FIGURE 1. Measured surface texture (a, left) and corresponding asperity height distribution (b, right)

THEORETICAL BACKGROUND

Numerical framework

A numerical friction framework has been developed to couple the various micro friction models. The friction model starts with defining the process variables and material characteristics. Process variables are the nominal contact pressure and strain in the material. Significant material characteristics are the hardness of the asperities and the surface properties of the tool and workpiece material. Once the input parameters are known, the real area of contact is calculated based on the models accounting for flattening due to normal loading and flattening due to stretching. The amount of indentation of the harder tool asperities into the softer workpiece asperities can be calculated if the real area of contact is known. After that, shear stresses due to ploughing and adhesion effects between asperities and the coefficient of friction are calculated. It is noted that in reality flattening due to normal loading and flattening due to stretching will appear simultaneously during sheet metal forming, as well as the combination between flattening and sliding. Nevertheless, it has been assumed that the various mechanisms act independently of each other in this research.

Characterization rough surfaces

Friction models encompassing micro-mechanisms are generally regarded as too cumbersome to be used in large-scale FE simulations. Therefore, translation techniques are necessary to translate microscopic contact behavior to macroscopic contact behavior. Using stochastic methods, rough surfaces are described on the micro-scale by their statistical parameters (asperity density, mean radius of asperities and the asperity height distribution). Assuming that the surface height distribution on the micro-scale represents the surface texture on the macro-scale, it is possible to describe contact problems that occur during large-scale FE analyses of sheet metal forming processes [4].

Figure 1a shows a 2 dimensional roughness measurement of an electrical discharged textured (EDT) steel material. The location of asperities and the asperity density can be obtained by using the nine-point summit rule [11, 12]. Summits are points with a local surface height higher than their 8 neighboring points. Once the location of the asperities is known and assuming that asperities are spherically tipped, the radius of the asperities is related to the local curvature at the surface. The curvature κ is defined as the second order derivative of the function, which can be obtained by the second order finite difference method [12]. The expressions given in Equation 1 can be used to obtain the radius β in two perpendicular directions and the equivalent radius. The expressions are based on the three point definition of a summit curvature in which $z_{x,y}$ represents the local surface height at the asperity location (x,y).

$$\kappa_{||} = \beta_{||}^{-1} = \frac{z_{x-1,y} - 2z_{x,y} + z_{x+1,y}}{\mathrm{d}x^2} \qquad \kappa_{\perp} = \beta_{\perp}^{-1} = \frac{z_{x,y-1} - 2z_{x,y} + z_{x,y+1}}{\mathrm{d}y^2} \qquad \kappa_{eq} = \beta_{eq}^{-1} = \frac{\kappa_{||} + \kappa_{\perp}}{2} \tag{1}$$

When using stochastic methods, only the mean radius of asperities is of interest:

$$\beta = \frac{1}{n_{asp}} \sum_{i}^{n_{asp}} \kappa_{eq,i}^{-1} \tag{2}$$

The histogram of all local asperities is called the asperity height distribution (Figure 1b). To describe the histogram a continuous function is desirable to eliminate the need for integrating discrete functions during the solution procedure of the friction model. Various methods exist to describe discrete signals by continuous functions. The Gauss distribution function can be used if it is assumed that the surface height distribution is symmetric and approximates a normal distribution function. However, the initial surface height distribution is usually asymmetric and will become even more asymmetric if there is flattening of contacting- and rising of non-contacting asperities. The asymmetric Weibull distribution function is a more flexible criterion but can only approximate smooth surface height distributions. A more advanced method to describe discrete signals can be achieved by using a Fourier series or by using B-splines. A Fourier series makes it possible to describe non-smooth asymmetric distribution functions from which the accuracy of the evaluation depends on the number of expansions used. Using B-splines, non-smooth asymmetric distribution functions can be evaluated from which the accuracy depends on the number of lines used to construct the curve. In Figure 1b, the asperity height distribution corresponding to the measured surface roughness (Figure 1a) is evaluated by a Gaussian, Weibull, Fourier and B-spline function. For the Fourier and B-spline function 10 Fourier expansions and 10 cubic lines were used, respectively. As can be seen, using a Gaussian or a Weibull function a large error in representing the histogram is introduced. A better evaluation can be obtained by using a Fourier series or a B-spline function, noting that the error could be reduced further by using more Fourier expansions or more lines to construct the B-spline. An advantage of the B-spline function, compared to the Fourier series, is that the derivative at the end points approaches zero, which can have a stabilizing effect in the friction algorithm. The Fourier series tends to oscillate towards the end points of the distribution when large tails are present, which represents unrealistic behavior and has a destabilizing effect on the friction algorithm. The computation time to solve the friction model, using the various distribution functions, will be discussed in the final section of this paper.

Flattening models

Two flattening mechanisms have been implemented in the friction model to calculate the real area of contact of the workpiece: flattening due to normal loading and flattening due to stretching. A non-linear plastic load model has been developed inspired by the ideal-plastic load model proposed by Westeneng [4, 13]. Besides an ideal-plastic load model, Westeneng proposed an ideal-plastic stretching model [4, 13] which has been used in this research. A brief explanation of the normal loading model is given in this paper, a detailed derivation of the model will be published in an upcoming paper.

Westeneng assumed the tool as rigid and perfectly flat, which indents into a soft and rough workpiece material. This assumption is valid since the difference in hardness and length scales between the tool and workpiece material is significant in the case of sheet metal forming processes. The asperities of the rough surface are modeled by bars which can represent arbitrarily shaped asperities, Figure 2. Westeneng introduced 3 stochastic variables as presented in Figure 2: The normalized surface height distribution function of the asperities of the rough surface $\phi(z)$, the uniform rise of the non-contacting surface U (based on volume conservation) and the separation between the tool surface and the mean plane of the asperities of the rough surface d.

Contact between a flat hard smooth surface and a soft rough surface is assumed without sliding and bulk deformation. Only plastic deformation of asperities is assumed including work-hardening effects. Using the normalized surface height distribution $\phi(z)$, expressions to obtain the amount of flattening of contacting asperities d and the rise of non-contacting asperities U can be obtained by energy and volume conservation laws:

$$P_{nom} = \frac{B}{\rho\omega}(\gamma + \eta\beta) \qquad U(1-\alpha) = \int_{d-U}^{\infty} (z-d)\,\phi(z)\,dz \qquad \text{with} \qquad \alpha = \int_{d-U}^{\infty} \phi(z)\,\mathrm{d}z \tag{3}$$

ρ represents the asperity density, ω can be regarded as an external energy factor while γ and β can be regarded as internal energy factors. ω, as well as γ and β are variables which depend on the statistical parameters U (the constant rise of asperities) and d (the separation between the tool surface and the mean plane of the asperities of the rough

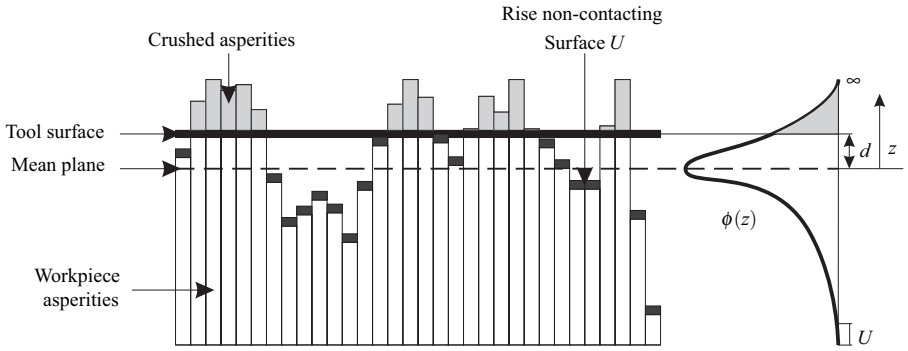

FIGURE 2. A rough soft surface flattened by a smooth rigid surface

surface). In addition, ω is a function of the normal forces acting on the asperities $F_N(z)$. It should be noted that an equal rise of asperities has been assumed in the derivation of ω, γ and β, which corresponds to the experimental results of Pullen & Williamson [8]. η represents the persistence parameter which describes the amount of energy required to lift up the non-contacting asperities. A value of $\eta = 0$ means that no energy is required to rise the asperities, a value of $\eta = 1$ implies that a maximum amount of energy is required to rise the asperities. Known parameters in Equation 3 are P_{nom}, the nominal contact pressure (input parameter), and B, a hardness parameter. Since non-linear plasticity is assumed, the hardness H of the softer material can be described by $H = B\sigma_Y$ (with B=2.8 for steel materials). The yield strength σ_y can be described by a flow rule which analytically describes the relation between the strain in the material and the yield strength of the material. A typical phenomenological model is the Nadai or Swift relation. The Nadai hardening function defines the yield stress σ_y as a function of the equivalent plastic strain ε_p and the strain at the initial yield stress ε_0:

$$\sigma_y = C\left(\varepsilon_p + \varepsilon_0\right)^n \qquad \text{with} \qquad \varepsilon_p = \begin{cases} \ln\left(\dfrac{\lambda + d - z}{\lambda}\right) & \text{for } z > d \\ \ln\left(\dfrac{\lambda + d - z}{\lambda}\right) & \text{for } d - U \le z < d \\ \ln\left(\dfrac{\lambda + U}{\lambda}\right) & \text{for } z \le d - U \end{cases} \tag{4}$$

in which C and n represents specific material characteristics and ε_p the logarithmic strain in the asperities. The strain in the asperities is defined as the amount of flattening or rise of asperities relative to the initial height of the asperities λ. In this respect, a definition for the strain can be derived for 1) asperities in contact with the indenter, 2) asperities which will come into contact due to the rise of asperities and 3) asperities which will not come into contact with the indenter (Equation 4). The model described above is based on a normal loading case without additional bulk strain. To account for flattening due to stretching, the model has to be adapted. The change of the fraction of the real contact area as a function of the nominal strain can be presented as:

$$\frac{\mathrm{d}\alpha_S^i}{\mathrm{d}\varepsilon} = \frac{l}{E}\phi\left(d_S^{i-1} - U_S^{i-1}\right) \tag{5}$$

with i the iteration number. The subscript S is used for variables that become strain dependent. The contact area ratio is updated incrementally by:

$$\alpha_S^i = \alpha_S^{i-1} + \mathrm{d}\alpha_S^i \tag{6}$$

The initial values α_S^0, d_S^0 and U_S^0 are obtained from the model without bulk strain. To calculate the change of α_S, the value of U_S and d_S needs to be solved simultaneously while ε is incrementally increased. Based on volume conservation and the definition of the fraction of real contact area (Equation 7) U_S and d_S can be obtained.

$$\alpha_S = \int_{d_S - U_S}^{\infty} \phi\left(z\right) dz \qquad\qquad U_S\left(1 - \alpha_S\right) = \int_{d_S - U_S}^{\infty} \left(z - d_S\right)\phi\left(z\right) dz \tag{7}$$

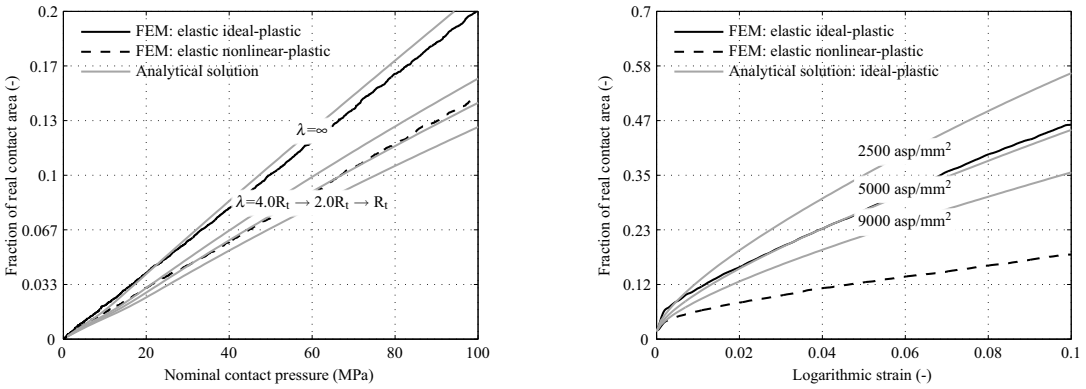

FIGURE 3. Development real contact area of analysis 1 (a, left) and development contact area of analysis 2 (b, right)

Shear stresses

The model of Challen & Oxley [2, 3] takes the combining effect of ploughing and adhesion between a wedge-shaped asperity and a flat surface into account. Westeneng [4] extended the model of Challen & Oxley to describe friction conditions between a flat workpiece material and multiple tool asperities. He assumed that the flattened peaks of the asperities are soft and perfectly flat and the surface of the tool material is rough and rigid. The difference in hardness between the tool and workpiece material and the difference in length scales between the two surfaces is significant in the case of a sheet metal forming process. Therefore, it is valid to make a subdivision in two length scales using a rigid tool and a soft workpiece. The extended version of Challen & Oxley's model [4] has been implemented in the friction model to describe friction conditions between the tool and workpiece material:

$$F_w = \rho_t \alpha_S A_{nom} \int_{\delta}^{s_{max}} \mu_{asp} \pi \omega \beta_t H \phi_t(s)\, ds \tag{8}$$

with ω the amount of indentation, β_t the mean radius of the tool asperities and μ_{asp} the coefficient of friction at single asperity scale [3]. ρ_t represents the asperity density of the tool surface, A_{nom} the nominal contact area and ϕ_t the normalized surface height distribution function of the tool surface. The bounds of the integral are described by s_{max}, the maximum height of the tool asperities, and δ, the separation between the workpiece surface and the mean plane of the tool asperities. Since the normal force is known (input parameter), the coefficient of friction can finally be obtained by:

$$\mu = \frac{F_w}{F_N} \tag{9}$$

VALIDATION

The newly developed non-linear load model as well as the ideal-plastic strain model of Westeneng have been validated by means of FE simulations on a two-dimensional rough surface. In the first analysis, a two-dimensional rough surface of 4mm long was deformed by a perfectly flat and rigid tool. The second analysis was focused on flattening a rough surface by a normal load including a bulk strain in the underlying material. Three simulations have been executed for each analysis using different roughness profiles. The roughness profiles equal three roughness measurements of DC04 low-carbon steel. The surface was modeled by 4 node 2D plane-strain elements. The yield surface was described by the Von Mises yield criterion using the Nadai hardening relation to describe work-hardening effects. The surface height distribution used for the analytical model corresponds to the roughness distribution of the FE simulation. The development of the real area of contact has been tracked during the simulation and compared with the analytical solution. Results shown in Figure 3 are the mean values of the three simulations performed per analysis case.

The non-linear load model uses the Nadai hardening relation to account for work hardening effects of the flattened asperities. An unknown parameter has been introduced during the derivation of this model: the initial height of

asperities λ (see Equation 4). Calculations have been performed using different values for this parameter: 1.0, 2.0 and 4.0 times the R_t value (Figure 3a). The R_t value represents the maximum peak to valley distance between asperities. The amount of strain build up in the asperities will be lower when using a higher value for the initial height λ. From the results, it can be concluded that the exact development of real contact area can be found when using an initial height of 2.0 times the R_t value. Increasing the initial height of asperities to infinity represents ideal plastic material behavior, since the strain build up in the material approaches zero. As shown in Figure 3a, the analytical solution describes the results of the ideal-plastic FE simulation well when using a value of $\lambda = \infty$.

Combined normal loading and stretching the underlying bulk material decreases the effective hardness [9]. A lower hardness results in an increase of the real area of contact. Both the analytical and the FE results of analysis 2, where a rough surface has been flattened by a nominal load and a bulk strain has been applied to the underlying material, are presented in Figure 3b. As for analysis 1, results shown are the mean values of three simulations performed per analysis case. It can be concluded that work-hardening effects have a large influence on the flattening behavior of the asperities.

The strain model developed by Westeneng uses the asperity density to obtain the flattening behavior of asperities. A line profile has been used in this section to generate the FE models. The asperity density of this profile has been obtained by the 3-point summit rule (1D version of the 9-point summit rule for surfaces). By taking the square of the asperity density found by the 3-point summit rule, a density of 2500 asp/mm^2 was found. Results obtained by the analytical strain model, using an asperity density of 2500, 5000 and 9000 asp/mm^2, are shown in Figure 3b. The trend of the graphs corresponds well, but the development of the real area of contact is significantly higher compared to the ideal-plastic FE results if an asperity density of 2500 asp/mm^2 is used. If a higher value of the asperity density is used the amount of real area of contact will be lower. Using an asperity density of 5000 asp/mm^2 it is possible to describe the results of the elastic ideal-plastic FE solution well.

IMPLEMENTATION

The developed friction model can be implemented in FE codes using two different strategies. One strategy is to implement the code of the friction model into the contact algorithm of the FE code. The friction model is called if a node of the workpiece comes in contact with the tool, resulting a friction coefficient belonging to that specific node. This strategy returns a specific coefficient of friction for each node in contact.

Another strategy is to initialize the coefficient of friction for a predefined range of process variables. Process variables are the nominal contact pressure and the bulk strain in the workpiece material. Since a rough guess can be made about the range of these variables a matrix can be constructed including friction values for all possible combinations. Figure 4a shows for example a friction matrix for a nominal contact pressure in between 0 and 100 MPa and a bulk strain in between 0 and 150%. The time required to construct this matrix, using various functions to evaluate the asperity height distribution, is shown in Figure 4b. The Gauss and Weibull distribution functions are the two fastest methods. However, the applicability of these methods is restricted by the relatively simple shape of the functions. Fourier series or B-splines could be used if more complex shapes are desired. The time required to build a friction matrix using Fourier series increases when increasing the number of Fourier expansions. The time required to construct a friction matrix using B-splines depends on the order of the B-spline (in this case cubic lines where used) instead of the number of lines used to construct the B-spline. Concerning the flexibility of the B-spline function and the numerical stability of the friction algorithm, the B-spline function is favorable in describing complex distributions. The Weibull distribution function is favorable in case of normally distributed distributions.

For the first strategy the friction routine is called for every node in contact each step of the simulation. Hence, this strategy can result in a huge increase of the simulation time. For the second strategy, the friction matrix has to be constructed only once. When the friction matrix is constructed it can be used during a FE simulation to find nodal friction values. Since only an interpolation scheme is required to find the nodal friction values, this method will hardly increase the simulation time. Difficulties with the second approach are however expected when it is desired to take history dependency of the deformed asperities into account. Loading/unloading and straining/unstraining of the workpiece material will take place during sheet metal forming which requires the use of history dependency. For the first strategy, friction values are calculated per step per node which makes it more straightforward to take the flattening history of previous steps into account.

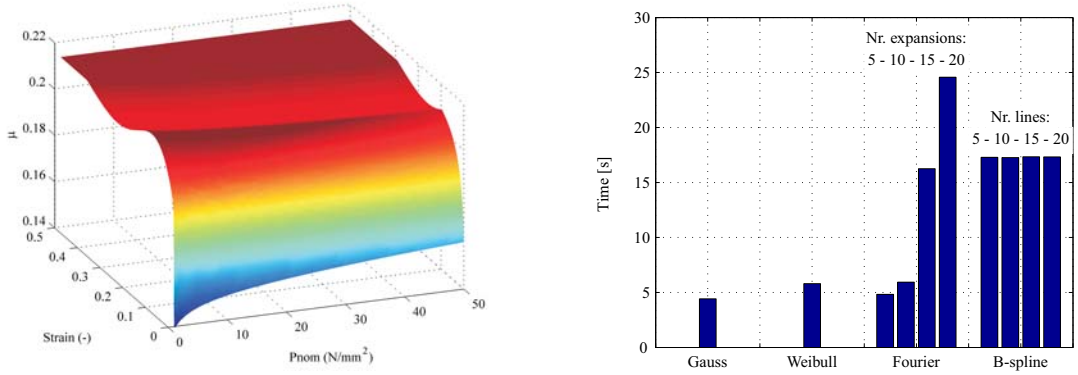

FIGURE 4. Friction matrix (a, left) and evaluation time using different distribution functions (b, right)

APPLICATION

A cross-die product is used to test the numerical performance of the developed friction model in a large-scale FE simulation (Figure 5a). Due to symmetry only a quarter of the workpiece was modeled. The workpiece was meshed with 9000 triangular discrete Kirchhoff shell elements using 3 integration points in plane and 5 integration points in thickness direction. The coefficient of friction used in the contact algorithm was calculated on the basis of the friction model presented in this paper. Simulations have been performed using both implementation strategies discussed in the previous section. A distribution of friction coefficients can be observed from the results presented in Figure 5a. Values of the friction coefficients are found ranging from 0.13 to 0.19. The gray area represents the non-contacting area.

It can be observed from Figure 5a that higher values of the coefficient of friction occur at regions where high strains occur (region A, B and C). Region A is purely stretched, region B is compressed which causes thickening of the material and region C is stretched over the die radius. Overall it can be concluded that the distribution of the coefficients of friction lies within the range of expectation.

The draw-in pattern of the simulation is compared to the simulation result in which the standard Coulomb friction model has been used with a friction coefficient of 0.13. It can be observed that the draw-in significantly deviates from the draw-in obtained with the Coulomb friction model. This is logical since the maximum obtained friction coefficient by the developed friction model is much higher than the fixed value of 0.13. When a fixed value of 0.19 is used, which is the maximum value found when using the developed friction model, failure of the cross-die will occur.

As mentioned before, simulations have been performed using two different strategies to couple the friction model to the FE code. Figure 5a shows the results obtained by using a friction matrix (the second strategy proposed). Results match perfectly with these obtained when using the first strategy (direct implementation of the friction algorithm in the contact algorithm of the FE code). However the simulation time grows significantly when using the first strategy. An increase of 3 times the simulation time required to perform a Coulomb based simulation was observed. On the other hand, an increase of less than 1% was observed when using the second strategy.

CONCLUSIONS

A friction model that can be used in large-scale FE simulations is presented. The friction model includes two flattening mechanisms to determine the real area of contact at a microscopic level. The real area of contact is used to determine the influence of ploughing and adhesion effects between contacting asperities on the coefficient of friction. A statistical approach is adapted to translate the microscopic models to a macroscopic level.

The friction model has been validated by means of FE simulations at a micro-scale. A good comparison was found between the FE simulations and the results obtained by the newly developed non-linear loading model. It has been shown that the non-linear load model can be used to describe both ideal-plastic and non-linear plastic material behavior. If a nominal strain is applied to the bulk material, the effect of work-hardening becomes significant. The ideal-plastic strain model is able to describe the trend of the FE results. However, it was not possible to accurately describe the

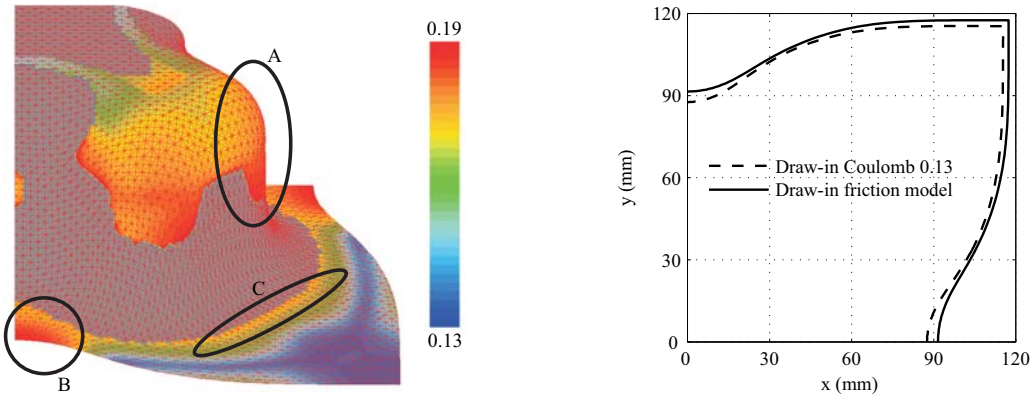

FIGURE 5. Development coefficient of friction cross die (a, left) and amount of draw-in (b, right)

ideal-plastic FE results, as well as the influence of work-hardening effects. Other, more advanced, models are required to accurately describe the influence of bulk straining on the flattening behavior of asperities.

The friction model could be directly implemented into FE codes or being coupled to the FE code by using a friction matrix. The first strategy requires to calculate nodal friction values each step of the simulation, which can result in a huge increase of the simulation time. When a friction matrix is used, only an interpolation scheme is required to find nodal friction values during the FE simulation which will result in a lower increase of the simulation time.

The friction model has been applied to a full-scale sheet metal forming simulation to test the numerical performance and feasibility of the developed friction model. The results look very promising. The modest increase in simulation time shows the feasibility of the friction model in large scale sheet metal forming simulations.

ACKNOWLEDGMENTS

This research was carried out under the project number MC1.07289 in the framework of the Research Program of the Materials innovation institute M2i (www.m2i.nl).

REFERENCES

1. W. Wilson, *Americal Society of Mechanical Engineers* **10**, 13–23 (1988).
2. J. Challen, and P. Oxley, *Wear* **53**, 229–243 (1979).
3. J. Challen, and P. Oxley, *International Journal of Mechanical Siences* **26**, 403–418 (1984).
4. J. Westeneng, *Modelling of contact and friction in deep drawing processes*, Ph.D. thesis, University of Twente (2001).
5. J. Greenwood, and J. Williamson, *Proceedings of the Royal Society of London. Series A, Mathematical and Physical sciences* **295**, 300–319 (1966).
6. Y. Zhao, and L. Chang, *Journal of Tribology* **123**, 857–864 (2001).
7. D. M. Y. Zhao, and L. Chang, *Journal of Tribology* **122**, 86–93 (2000).
8. J. Pullen, and J. Williamson, *Proceedings of the Royal Society of London. Series A, Mathematical and Physical sciences* **327**, 159–173 (1972).
9. W. Wilson, and S. Sheu, *International Journal of Mechanical Science* **30**, 475–489 (1988).
10. M. Sutcliffe, *International Journal of Mechanical Science* **30**, 847–868 (1988).
11. J. Greenwood, *Proceedings of the Royal Society of London. Series A, Mathematical and Physical sciences* **393**, 133–157 (1984).
12. M. de Rooij, *Tribological aspects of unlubricated deepdrawing processes*, Ph.D. thesis, University of Twente (1998).
13. J. Hol, M. C. Alfaro, M. de Rooij, and T. Meinders, *WEAR* (2010, doi:10.1016/j.wear.2011.04.004).